Chamchuri Journal of Mathematics
Volume 8(2016), 18–33
http://www.math.sc.chula.ac.th/cjm

The effect of inverted cone inserts design on granular behavior in silo

Wariam Chuayjan*, Sutthiwat Thongnak and Benchawan Wiwatanapataphee

Received 10 May 2016
Revised 29 May 2017
Accepted 10 June 2017

Abstract: This paper proposes to study the effect of the insert design on behavior of granular flow during silo discharge. The mathematical model based on the principle of linear momentum and angular momentum for the motion of granular during silo discharge is presented. Discrete Element Method is applied to obtain the solution of the model. The silo with an inverted cone insert is used in this study. The impact of three different vertex angles of the insert including $30°, 60°$ and $90°$ and four locations of the insert on flow pattern, velocity and wall pressure of granular flow during discharging process are investigated. The results show that the mathematical model can capture the granular behavior in the silo. The vertex angles and positions of the insert have significant effects on the flow pattern, the velocity field and wall pressure in the silo.

Keywords: inverted-cone-shaped insert, silo, granular material, flow pattern, Discrete Element Method

2000 Mathematics Subject Classification: 83C10

* *Corresponding author*

1 Introduction

A silo is a bulk storage container for the transport of industrial goods such as sand, soybean, nuts, rice, coffee, cornflakes, powders etc. There are many types of silo such as bin, hopper and tank used in industries for different purposes serving different types of industries. Capacity of the silo can vary from less than 1 tons to 100,000 tons, so the silo design must be considered to meet the requirement of structural safety and well-functioning. Understanding of granular behavior, wall pressure and other factors affecting the flow in a bin storage during discharge process is essential.

Over a last century, the granular behavior in the silo has been extensively studied. There are two different ways of study including experimental model and numerical model. The first study was done by Roberts in 1882 (see [15]). He calculated pressure distribution in a rectangular silo using a mathematical expression. Janssen (see [9]) and Reimbert (see[14]) proposed a mathematical formulae to calculate pressure inside the silo. However, the simplistic research procedures cannot be used to correctly describe behavior of the granular in the silo because there are many factors such as properties of granular material, silo geometry, displacing insert and surface friction of the silo wall. During the discharging process, when the outlet is opened, fine particles start to flow under gravity from silo. To describe this complex situations, numerical techniques have been developed for investigation of granular behavior and pressure in the silo. Two numerical techniques including Finite Element Method (FEM) and Discrete Element Method (DEM) have been employed to cope with a variety of issues during the discharge process. In FEM, the granular material is assumed as a continuum. The mathematical models of granular flow based on FEM give approximate solutions for prediction of complex phenomena such as pressure distribution in the bin storage, pressure on the wall and flow pattern (see [6], [18] and [20]). However, this method neglects the discontinuity of granular mass and cannot simulate some conditions such as the collision of particles. Another method for simulating of movement of particulate particles is the DEM (see [5]). The method allows managing variables controlling the behavior of granular materials.

Recently, many researches have used the DEM to describe the pressure distribution (see [3] and [7]), the flow pattern (see [4] and [8]), the flow rate (see [1] and [12]), the segregation and the arching problem (see [11] and [13]) during the discharge process. It is noted that there are two main flow patterns including

the funnel-shaped flow and the bulk flow occurred during silo discharge. In the funnel-flow situation, granular material in the middle part of the silo and above orifice flows out from the silo but the material along the wall remains stationary. In other situations, all material is in motion. The flow patterns depend on the properties of granular material and the silo construction. Generally, an insert is placed in the silo for improving the flow pattern, eliminating stagnant zone (see [2] and [17]) and decreasing flow pressure (see [16] and [19]) and discharge rates (see [10] and [19])).

In this paper, a Discrete Finite Element Model is proposed to investigate effects of vertex angle and the position of an inverted-cone-shaped insert on the granular behaviors. The mathematical model of particulate flow is presented in section 2. By Numerical solutions including flow pattern, velocity field, and pressure are presented in section 3. Finally, the conclusion is given in section 4.

2 Mathematical Model

The mathematical model based on the principle of linear momentum and angular momentums is established to compute the velocities and positions of all particles. When force and moment act on the particle i, translational/rotational motion may occur. The governing equations describing movement of the particle i are given as follows:

$$m_i\ddot{\boldsymbol{r}}_i(t) = m_i\mathbf{g} + \mathbf{F}_i(t), \tag{1}$$

$$I_i\ddot{\boldsymbol{\theta}}_i(t) = \mathbf{M}_i(t), \tag{2}$$

where m_i and I_i denote the mass and the moment of inertia of the particle i , $\mathbf{g}$ is gravititional force and $\boldsymbol{r}_i(t)$, $\boldsymbol{\theta}_i(t)$ represent vectors of the position and angular rotation at the centre of the particle i, respectively. $\mathbf{F}_i(t)$ and $\mathbf{M}_i(t)$ are the total force and torque acting on the particle i at time t, respectively.

The equation describing the total force is defined by

$$\mathbf{F}_i(t) = \sum_{j=1,\, j\neq i}^{N_p} \mathbf{F}_{i,j} + \sum_{k=1}^{N_w} \mathbf{F}_{i,w_k}, \tag{3}$$

where N_p and N_w are respectively the number of contact particles and walls

acting on the particle i. $\mathbf{F}_{i,j}$ and $\mathbf{F}_{i,w_k}$ are determined by

$$\mathbf{F}_{i,j}(t) = F_{ijn}(t)\mathbf{n} + F_{ijs}(t)\mathbf{s}, \tag{4}$$

$$\mathbf{F}_{i,w}(t) = F_{iwn}(t)\mathbf{n} + F_{iws}(t)\mathbf{s}, \tag{5}$$

where F_{ijn} is the normal force and F_{ijs} is the shearing force acting on the particle, F_{iwn} and F_{iws} are the forces in the normal and tangential directions of the wall contact plane, repectively. $\mathbf{n}$ and $\mathbf{s}$ are the unit vectors in the normal and tangential directions of the contact plane.

For the total torque, we denote

$$\mathbf{M}_i(t) = \sum_{j=1,\, j\neq i}^{N_p} \boldsymbol{r}_i \times \mathbf{F}_{i,j} + \sum_{k=1}^{N_w} \boldsymbol{r}_i \times \mathbf{F}_{i,w_k}. \tag{6}$$

Let $\boldsymbol{v}_i(t) = \dot{\boldsymbol{r}}_i(t)$ and $\boldsymbol{\omega}_i(t) = \dot{\boldsymbol{\theta}}_i(t)$ for $i = 1, 2, 3, ..., N_p$.

Then, we obtain a system of first order ordinary differential equations

$$\begin{array}{rcl} \dot{\boldsymbol{r}}_i(t) & = & \boldsymbol{v}_i(t), \\ \dot{\boldsymbol{\theta}}_i(t) & = & \boldsymbol{\omega}_i(t), \\ \dot{\boldsymbol{v}}_i(t) & = & \frac{\mathbf{g}+\mathbf{F}_i(t)}{m_i}, \\ \dot{\boldsymbol{\omega}}_i(t) & = & \frac{\mathbf{M}_i(t)}{I_i}. \end{array} \tag{7}$$

The above system is extended to describe the movement of all particles, and becomes

$$\dot{\boldsymbol{\psi}}(t) = \boldsymbol{\phi}(t), \tag{8}$$

$$\dot{\boldsymbol{\phi}}(t) = \boldsymbol{F}(t), \tag{9}$$

where $\boldsymbol{\psi}(t)$, $\boldsymbol{\phi}(t)$ and $\boldsymbol{F}(t)$ are vectors defined as

$$\begin{array}{rcl} \boldsymbol{\psi}(t) & = & [\boldsymbol{r}_1(t) \quad \boldsymbol{\theta}_1(t) \quad ... \quad \boldsymbol{r}_{N_p}(t) \quad \boldsymbol{\theta}_{N_p}(t)]^T, \\ \boldsymbol{\phi}(t) & = & [\boldsymbol{v}_1(t) \quad \boldsymbol{\omega}_1(t) \quad ... \quad \boldsymbol{v}_{N_p}(t) \quad \boldsymbol{\omega}_{N_p}(t)]^T, \\ \boldsymbol{F}(t) & = & [\frac{\mathbf{g}+\mathbf{F}_1(t)}{m_1} \quad \frac{\mathbf{M}_1(t)}{I_1} \quad \frac{\mathbf{g}+\mathbf{F}_{N_p}(t)}{m_{N_p}} \quad \frac{\mathbf{M}_{N_p}(t)}{I_{N_p}}]^T. \end{array} \tag{10}$$

To find the numerical solution, the central difference scheme is applied to equations (8) and (9). Over the time interval $\Delta t = [t_{N-\frac{1}{2}}, t_{N+\frac{1}{2}}]$, equation (9) yields

$$\frac{\boldsymbol{\phi}^{N+\frac{1}{2}} - \boldsymbol{\phi}^{N-\frac{1}{2}}}{\Delta t} = \boldsymbol{F}^N. \tag{11}$$

Thus,

$$\boldsymbol{\phi}^{N+\frac{1}{2}} = \boldsymbol{\phi}^{N-\frac{1}{2}} + \boldsymbol{F}^N \Delta t. \tag{12}$$

Over the time interval $\Delta t = [t_N, t_{N+1}]$, further application of the central difference scheme to equation (8) at time $t_{N+\frac{1}{2}}$ gives,

$$\frac{\boldsymbol{\psi}^{N+1} - \boldsymbol{\psi}^{N}}{\Delta t} = \boldsymbol{\phi}^{N+\frac{1}{2}}, \tag{13}$$

or

$$\boldsymbol{\psi}^{N+1} = \boldsymbol{\psi}^{N} + \boldsymbol{\phi}^{N+\frac{1}{2}} \Delta t. \tag{14}$$

By substituting equation (12) into equation (14), one can obtain new translational and rotational displacements at time $t = N + 1$ as follows

$$\boldsymbol{\psi}^{N+1} = \boldsymbol{\psi}^{N} + \boldsymbol{\phi}^{N-\frac{1}{2}} \cdot \Delta t + \boldsymbol{F}^{N} \cdot (\Delta t)^2. \tag{15}$$

The new translational and rotational velocities, $\boldsymbol{v}_i(t)$ and $\boldsymbol{\omega}_i(t)$, at $t = N + 1$ are determined by

$$\frac{d}{dt}(\boldsymbol{\psi}^{N+1}) = \boldsymbol{\phi}^{N+1}. \tag{16}$$

3 Numerical Results

In previous section, we present the mathematical model based on the Discrete Element formultion. The model allows to analyse the effect of the vertex angles and the positions of an inverted-cone-shaped insert. In our simulation, the silo is made of steel-sheet with 30° of hopper angles (α). The height and width of the silo are $0.7\,m$ and $0.4\,m$, respectively. The outlet width is $0.08\,m$. To investigate the pressure along the bottom wall, pressure distribution on the hopper bottom is recorded at 10 positions at s_1 to s_{10} as shown in Figure 1(b). Figure 1(a) and 1(c) show the geometry of the silo with an inverted-cone-shaped insert and the four locations of the insert above the orifice, respectively.

For the study of the effect of the insert geometry, we consider the vertex angle and the position of the insert. The inverted-cone-shaped insert is placed at $0.06\,m$ above the orifice. The vertex angles (θ) of the insert are 30°, 60° and 90° and the length of insert base (r) is $0.04\,m$. To investigate the effect of insert position, the insert with 60° of the vertex angle is placed at four levels including levels A, B, C and D which are $0.04\,m, 0.06\,m, 0.08\,m$ and $0.1\,m$ above the orifice, repectively. At the point A, the insert body is in the hopper region. At points B and C, the insert is placed in the transition region between the hopper and the bin. At the point D, the whole insert is located in the bin regime. The number of particles

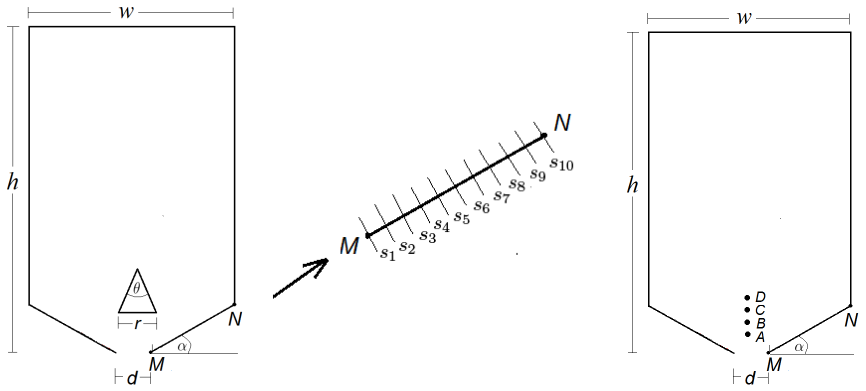

(a) (b) (c)

Figure 1: Geometry of silo: (a) a cylinder-hopper silo with an inverted-cone-shaped insert, (b) wall segments of the silo bottom and (c) the insert positions at A, B, C and D.

in the simulation is totally $4,000$ particles. The particles are spherical shape with two different diameters including $0.006\,m$ and $0.0075\,m$. The parameter values for calculation of the velocity field and pressure field are presented in Table 1 and the properties of the granular solids including normal contact stiffness, normal damping constant, tangential contact stiffness and frictional coefficient are presented in Table 2 .

3.1 The Effect of vertex angles of an inverted-coned-shaped insert in the silo

In this section, the effect of vertex angle on flow behavior is investigated. The computed flow patterns, velocity fields, and wall pressure distributions are presented in Figures 2, 3, 4, 5, 6, 7, 8 and 9. To investigate the flow pattern during silo discharge, all particles in the silo are allowed to flow through the outlet under gravity at $t \geq 0\,s$. To analyze the flow pattern of the granular material in the silo during discharge process, we introduce two different colors highlighted to the granular material as shown in Figure 2(a).

The deformation of the interface and velocity field of granular flow in the silo with three insert-vertex angles of $30°$, $60°$ and $90°$ as shown in Figures 2, 3 and

Table 1: Parameter values used in the simulation

Parameters	Value
Number of particles	$4,000$
Particle diameter	$0.006\,m$ and $0.0075\,m$
Particle density, ρ	$1,033\,kg/m^3$
Silo height, h	$0.7\,m$
Silo weight, w	$0.4\,m$
Outlet width, d	$0.08\,m$
Vertex angle of inverted cone insert, θ	$30^\circ, 60^\circ$ and 90°
Simulation time step, Δt	$5.2711 \times 10^{-6} s$

Table 2: Properties of particle

Properties	Particle-particle	Particle-wall
Normal contact stiffness, k_n	$2.8322 \times 10^4 N/m$	$5.6645 \times 10^4 N/m$
Normal damping constant, η_n	$1.3048 \times 10^2 N/m$	$1.3962 \times 10^2 N/m$
Tangential contact stiffness, k_s	$2.5740 \times 10^4 N/m$	$4.5314 \times 10^4 N/m$
Frictional coefficient, μ	0.33	0.35

4, respectively. The results indicate that the interfaces of the granular flow are V-shape and the outflow rates of granular obtained from the models with $\theta = 30°$, $\theta = 60°$ and $\theta = 90°$ of the vertex angle are not different.

The velocity field of granular solids in the silos are illustrated in Figure 5. The normal pressure acting along 10 segments of the hopper wall and average normal pressure are presented in Figures 6, 7, 8 and 9. The results show that the silo with $\theta = 90°$ of the insert gives the smallest low-speed zone while the one with $\theta = 30°$ of the insert gives the largest low-speed zone . For pressure distribution, the maximum can be found on hopper wall next to the bin wall (section 10). The lowest and highest average normal pressure appear in silo with $\theta = 90°$ and $\theta = 60°$ of the insert, respectively.

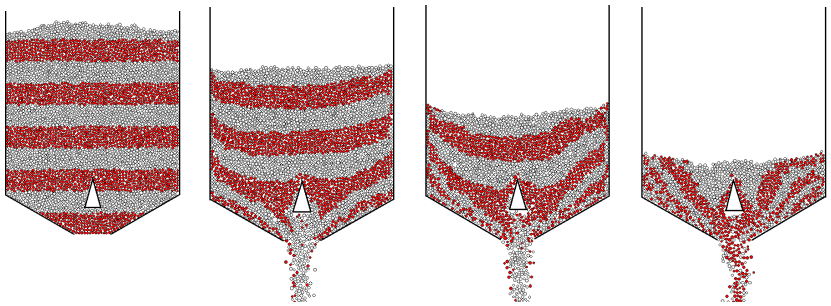

(a) $t = 0\,s$ (b) $t = 25\,s$ (c) $t = 50\,s$ (d) $t = 75\,s$

Figure 2: Flow pattern of granular material in the silo with $30°$ of vertex angle of the insert at different times.

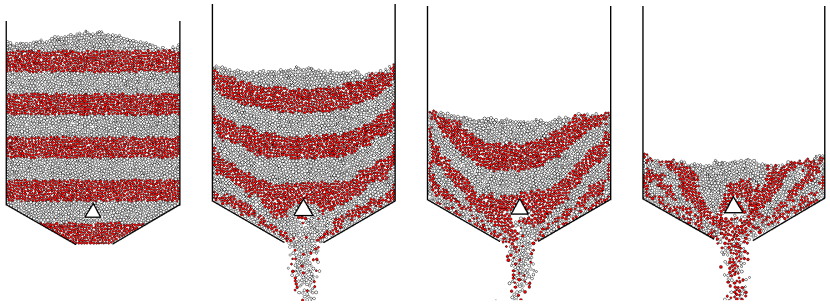

(a) $t = 0\,s$ (b) $t = 25\,s$ (c) $t = 50\,s$ (d) $t = 75\,s$

Figure 3: Flow pattern of granular material in the silo with 60° of vertex angle of the insert at different times.

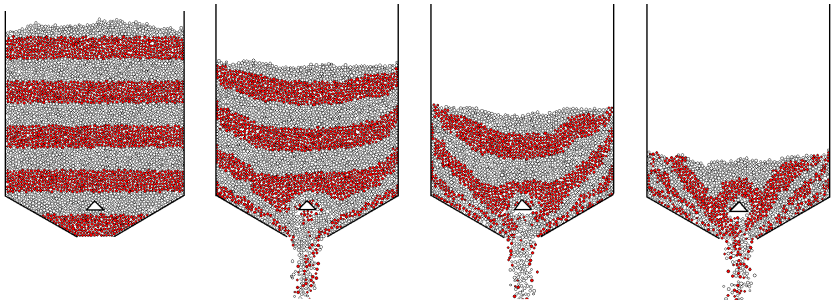

(a) $t = 0\,s$ (b) $t = 25\,s$ (c) $t = 50\,s$ (d) $t = 75\,s$

Figure 4: Flow pattern of granular material in the silo with 90° of vertex angle of the insert at different times.

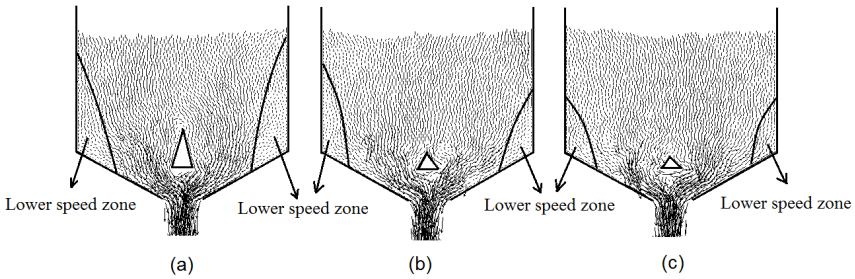

Figure 5: Velocity field of granular material in the silo with three different vertex angles (θ) of the insert at $t = 40\,s$: (a) $\theta = 30^\circ$, (b) $\theta = 60^\circ$ and (c) $\theta = 90^\circ$.

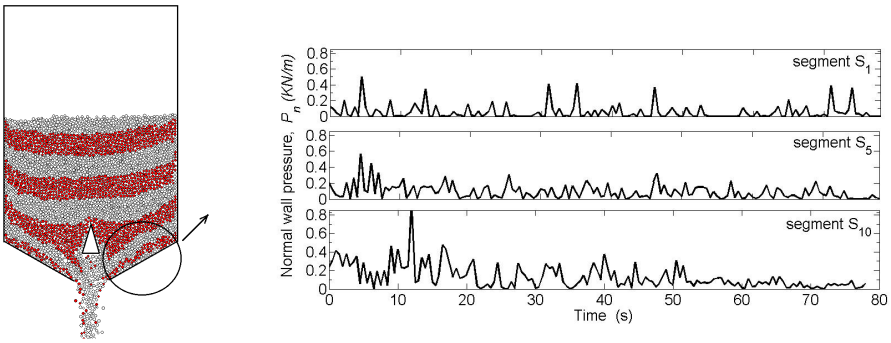

Figure 6: Normal wall pressure of granular material in the silo with $\theta = 30°$ of vertex angles of the insert during the first $80\,s$ of discharge process.

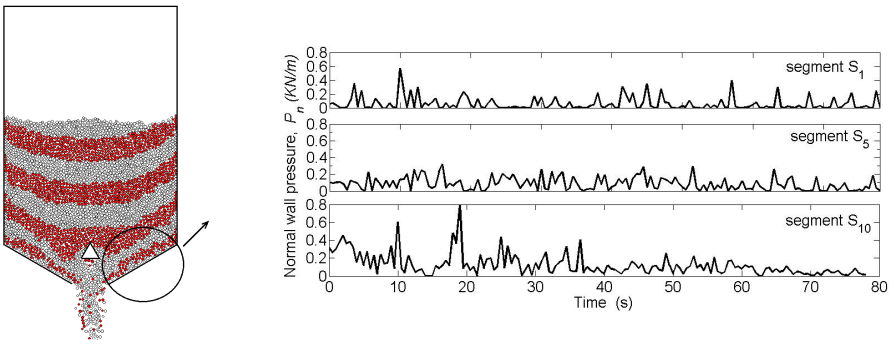

Figure 7: Normal wall pressure of granular material in the silo with $\theta = 60°$ of vertex angles of the insert during the first $80\,s$ of discharge process.

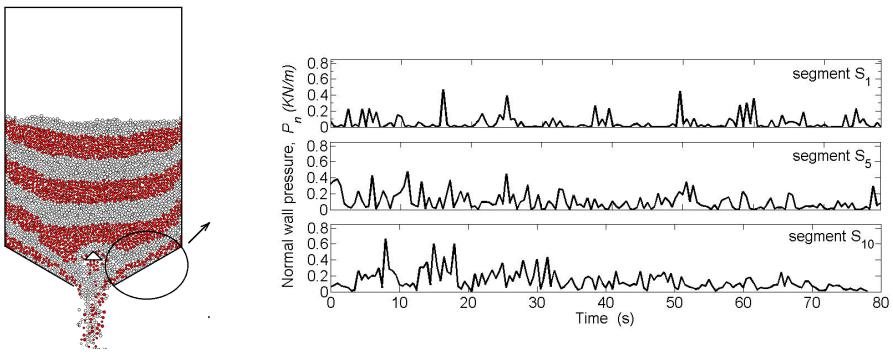

Figure 8: Normal wall pressure of granular material in the silo with $\theta = 90°$ of vertex angles of the insert during the first $80\,s$ of discharge process.

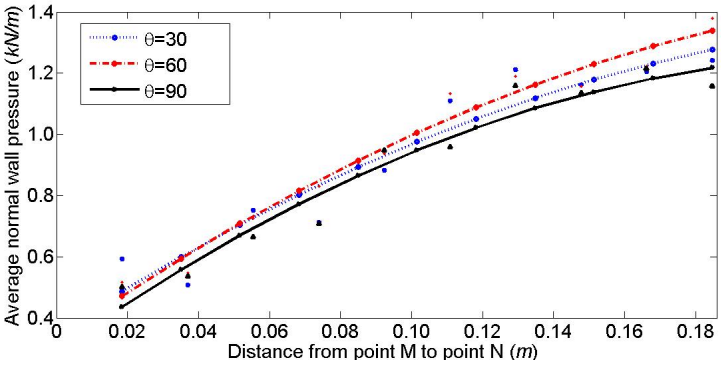

Figure 9: Avearge normal wall pressure along the hopper wall of the silo with $\theta = 30°$, $\theta = 60°$ and $\theta = 90°$ of vertex angle of the insert during the first $80\,s$ of discharge process.

3.2 The Effect of position of an inverted-cone-shaped insert in the silo

In this section, the effect of position of the inverted-cone-shaped insert is investigated. Four different computational domains of silo have been used to analyze the flow pattern, the velocity profile, and the pressure distribution. The computed flow pattern and the velocity field are presented in Figures 10 and 11, respectively. The results show that the movement interfaces of particles in those four silos are

V-shape. The silo with the insert located at level D gives the smallest low-speed zone, but the largest low-speed zone appears in one with the insert located at level A.

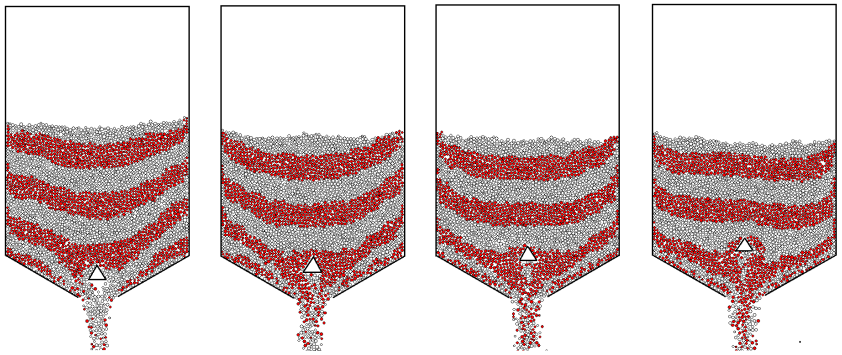

Figure 10: Discharge pattern at $t = 35\,s$ obtained from the silo with an inverted cone insert placing at 4 different locations above the orifice: (a) level A ($0.04\,m$), (b) level B ($0.06\,m$), (c) level C ($0.08\,m$) and (d) level D ($0.10\,m$).

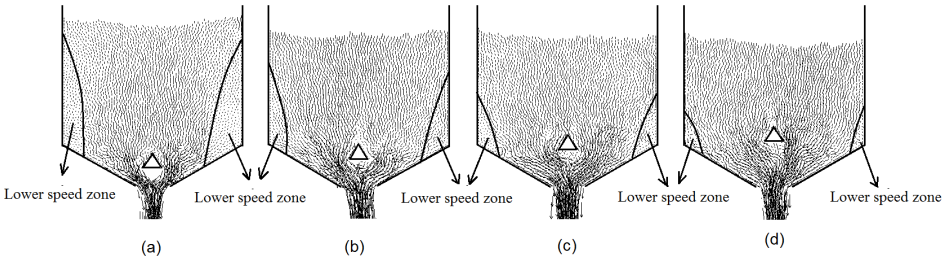

Figure 11: Velocity field of granular materials at $t = 35\,s$ obtained from the silo with an inverted cone insert placing at 4 different locations above the orifice: (a) level A ($0.04\,m$), (b) level B ($0.06\,m$), (c) level C ($0.08\,m$) and (d) level D ($0.10\,m$).

The computed average normal pressures are presented in Figure 12. The result shows that the average normal wall pressure in those four silos with different positions of the insert seem to be linear increasing. The highest average normal wall pressure appears in the silo with the insert located at the level A, while the

lowest wall pressure occurs in the one with the insert located at the level D.

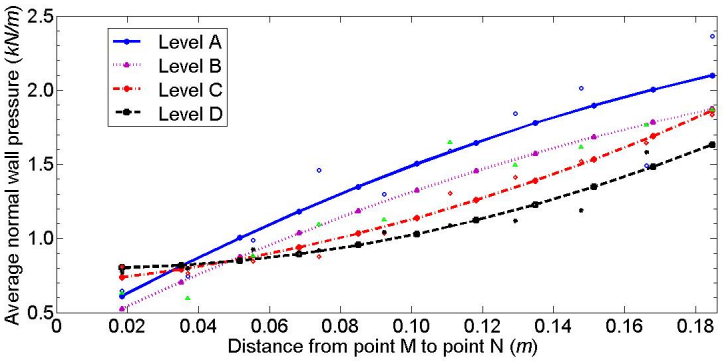

Figure 12: Avearge normal wall pressure along the hopper wall (from point M to N in Figure 1) during the first $80\,s$ of discharge process.

4 Conclusion

This paper presents the mathematical model and numerical simulation based on Discrete Element Method to capture the dynamic behavior of granular material inside the silo. The simulation allows to study the effect of different vertex angles and positions of the inverted-cone-shaped insert installed in silo. When the insert is placed in the silo, the flow patterns seem to be mass flow because all particles are in motion. There is no aching occurred in the simulation. For studying the effect of vertex angle of the insert, we found that the average normal pressure in the silo with $\theta = 90^\circ$ of the insert is lowest, but the pressure in the silo with $\theta = 60^\circ$ of insert is highest. For the study of the effect of position of insert in silo, it is found that the highest pressure appears when the insert is located at level A, while the lowest pressure occurs when the insert is located at the level D.

Acknowledgements: The authors gratefully acknowledge the financial support from Thaksin University Research Fund.

References

[1] R. Balevicius, I. Sielamowicz, Z. Mroz and Kacianauskas, Investigation of wall stress and outflow rate in a flat-bottomed bin: A comparison of the DEM model results with the experimental measurements, *Powder technology*, **214(3)**(2011), 322–336.

[2] C.S. Chou, A.F. Lee, and C.K. Yeh, Placement of a non-isosceles-triangle insert in an asymmetrical two-dimensional bin-hopper, *Advanced Powder Technology*, **20**(2009), 80–88.

[3] W. Chuayjan, S. Pothiphan, B. Wiwatanapataphee and Y.H. Wu, Numerical simulation of granular flow during filling and discharging of a silo, *International Journal of Pure and Applied Mathematics*, **62(3)**(2009), 347–364.

[4] W. Chuayjan, P. Boonkrong and B. Wiwatanapataphee, Effect of the silo-bottom design on the granular behavior during discharging process, *Proceeding of the 11th WSEAS International Conference on System Science and Simulation in Engineering(ICOSSSE'12), Singapore, May*, (2012), 68–73.

[5] P.A. Cundal and O.D.L. Strack, A discrete numerical model for granular assemblies, *Geotechnique*, **29**(1979), 47–65.

[6] S. Ding, M. Wójcik and M. Jecmenica, Loads on walls and inserts in a mass-flow silos, *TASK Quarterly: scientific bulletin of Academic Computer Centre in Gdansk*, **7**(2003), 525–538.

[7] T.J. Goda and F. Ebert, Three-dimensional discrete element simulations in hoppers and silos, *Powder technology*, **158(1)**(2005), 58–68.

[8] C. González-Montellano, F. Ayuga and J.Y. Ooi, Discrete element modelling of grain flow in a planar silo: influence of simulation parameters, *Granular Matter* **13(2)**(2011), 149–158.

[9] H.A. Janssen, Versuuch über Getreidedruck in Sillozellen, *Zeitschrift des Vereins Deutscher Ingenieure*, **39**(1895), 1045–1049.

[10] J.R. Johanson and W.K. Kleysteuber, Flow corrective inserts in bins, *Chemical Engineering Process* , **11(62)**(1966), 79–83.

[11] W.R. Ketterhagen, J.S. Curtis, C.R. Wassgren, A. Kong, P.J. Narayan and B.C. Hancock, Granular segregation in discharging cylindrical hoppers: a discrete element and experimental study, *Chemical Engineering Science*, **62(22)**(2007), 6423–6439.

[12] C. Mankoc, A. Janda, R. Arevalo, J.M. Pastor, I. Zuriguel, A. Garcimartn, and D. Maza, The flow rate of granular materials through an orifice, *Granular Matter*, **9(6)**(2007), 407–414.

[13] S. Masson and J. Martinez, Effect of particle mechanical properties on silo flow and stresses from distinct element simulations, *Powder Technology*, **109(1)**(2000), 164–178.

[14] M. Reimbert and A. Reimbert, Silos-Traité Theorique et Pratique, *Paris:Enrolles*, (1956).

[15] I. Roberts, Pressure of stored grain, *Engineering*, **34**(1882), 399.

[16] D. Schulze, Silos-Design variants and special types, *Bulk Solids Handling*, **16(2)**(1996), 225–232.

[17] S. Volpato, R. Artoni, and A.C Santomaso, Numerical study on the behavior of funnel flow silos with and without inserts through a continuum hydrodynamic approach, *Chemical Engineering Research and Design*, (2007).

[18] M. Wjcik and J. Tejchman, Numerical simulations of granular material flow in silos with and without insert, *Archives of Civil Engineering*, **53(2)**(2007), 293–322.

[19] S.C. Yang and S.S. Hsiau, The simulation and experimental study of granular materials discharged from a silo with the placement of inserts, *Powder Technology*, **120**(2001), 244–255.

[20] O.C. Zienkiewicz and R.L. Taylor, *The finite element method*,(6th ed.), United Kingdom:Butterworth-Heinemann Ltd.

Wariam Chuayjan
Department of Mathematics and Statistics,
Faculty of Science, Thaksin University,

Phatthalung Campus, Paphayom
Phatthalung, 93210,
Thailand
Email: cwariam@tsu.ac.th

Sutthiwat Thongnak
Department of Mathematics and Statistics,
Faculty of Science, Thaksin University,
Phatthalung Campus, Paphayom
Phatthalung, 93210,
Thailand
Email: tsutthiwat@tsu.ac.th

Benchawan Wiwatanapataphee
Department of Mathematics and Statistics,
Curtin University of Technology,
Perth, WA, 6845,
Australin
Email: B.wiwatanapataphee@curtin.edu.au